Smart Structures and Systems, Vol. 4, No. 5 (2008) 685-696
DOI: http://dx.doi.org/10.12989/sss.2008.4.5.685

Design of a bracing-friction damper system for seismic retrofitting

Sung-Kyung Lee

Department of Architectural Engineering, Dankook University, Seoul, Korea

Ji-Hun Park

Department of Architectural Engineering, University of Incheon, Incheon, Korea

Byoung-Wook Moon, Kyung-Won Min* and Sang-Hyun Lee

Department of Architectural Engineering, Dankook University, Seoul, Korea

Jinkoo Kim

Department of Architectural Engineering, Sungkyunkwan University, Korea

(Received March 20, 2007, Accepted December 11, 2007)

Abstract. This paper deals with the numerical model of a bracing-friction damper system and its deployment using the optimal slip load distribution for the seismic retrofitting of a damaged building. The Slotted Bolted Connection (SBC) type friction damper system was tested to investigate its energy dissipation characteristic. Test results coincided with the numerical ones using the conventional model of a bracing-friction damper system. The placement of this device was numerically explored to apply it to the assumed damaged-building and to evaluate its efficiency. It was found by distributing the slip load that minimizes the given performance indicies based on structural response. Numerical results for the damaged building retrofitted with this slip load distribution showed that the seismic design of the bracing-friction damper system under consideration is effective for the structural response reduction.

Key words: bracing-friction damper system; slotted bolted connection type; slip load distribution; damaged building.

1. Introduction

Passive energy dissipation devices such as visco-elastic dampers, metallic dampers and friction dampers have widely been used to reduce the dynamic response of civil engineering structures subjected to seismic loads. Their effectiveness for sesmic design of building structures is attributed to minimizing structural damages by absorbing the structural vibratory energy and by dissipating it through their

*Corresponding author, E-mail: kwmin@dankook.ac.kr

inherent hysteresis behavior (Soong, *et al*. 1997). Among these dampers, friction dampers with various designs have been developed and applied for the seismic protection of building structures since their hysteretic behaviors could be kept stable for cyclic loads and desirable slip loads are easily obtained by regulating normal forces acting perpendicularly to a friction surface, in addition to their simple energy dissipation mechanism and easy manufacturing, installation and maintenance (Pall and Marsh 1982, Consstantinou, *et al.* 1990, Grigorian, *et al*. 1992, Li and Reinhorn 1995, Mualla and Belev 2002).

For the application of these friction dampers to a seismic design of building structures, to begin with their slip loads and the stiffness of supporting braces should be determined. Filatrault and Cherry have proposed the design procedure of friction dampers that minimizes the sum of the displacement and dissipating energy by carrying out the parameter studies such as the structural fundamental period, frequency components of excitation load and the slip load of friction damper (Filiatrault and Cherry 1990). Fu and Cherry have designed the friction damper by using a force normalization coefficient (Fu and Cherry 2000). Garcia and Soong have proposed the method that obtains the optimal viscosity in terms of a story distribution by iterating the process that the inter-story drift or the inter-story velocity is defined as a controllable index and then installs the viscous damper at the location of maximum contollable index (Garcia and Soong 2002). Moreschi and Singh have determined the optimal slip load and the bracing stiffness by using the optimization technique such as genetic algorithm (Moreschi and Singh 2003). Viti, *et al*. proposed both the weakening retrofit to reduce maximum acceleration and the supplemental damping devices to control structural deformations (Viti, *et al*. 2006). They also performed inelastic spectral analysis to verify the proposed retrofitting strategy. Syrmakezis et al. investigated the retrofitting of hospital buildings by using the method of increasing the strength of a building and by applying visco-elastic dampers for the increase of the stability of the structure (Syrmakezis, *et al*. 2006).

However, many of these studies have been focused on the seismic design of new buildings or the seismic retrofit of existing buildings for the purpose of conforming to the strengthening of seismic codes to provide against increasing seismic hazard.

This paper discusses the seismic design of the friction damper using performance indicies of the controlled structural response in aspect of seismic retrofit of aged or damaged building structures. In this paper, first the Slotted Bolted Connection (SBC) type friction damper system that comprises steel braces and brass plates is tested for monotonic and cyclic loads to investigate its energy dissipation characteristic. Test results are compared with numerical results based on the conventional braced friction damper model to evaluate its applicability to seismic retrofit. Then, the placement of this device is numerically investigated to apply it to the assumed damaged-building and to evaluate its efficiency. Finally, the optimal slip load, which minimizes the given performance indicies based on structural response such as an acceleration and inter-story drift, is found and the efficacy of SBC type friction damper system under consideration is evaluated.

2. Performance test of a bracing-friction damper system

2.1. Test set-up

Brass is widely used as the metal that induces friction forces of SBC type friction dampers due to their high corrosion resistance and thus its maintenance such as a keeping the slip load during the life cycle of a structure (Grigorian, *et al*. 1993). In this study, SBC type friction damper system was tested using brass and steel plates that induce friction forces of the damper. Fig. 1(a) shows the brass and steel

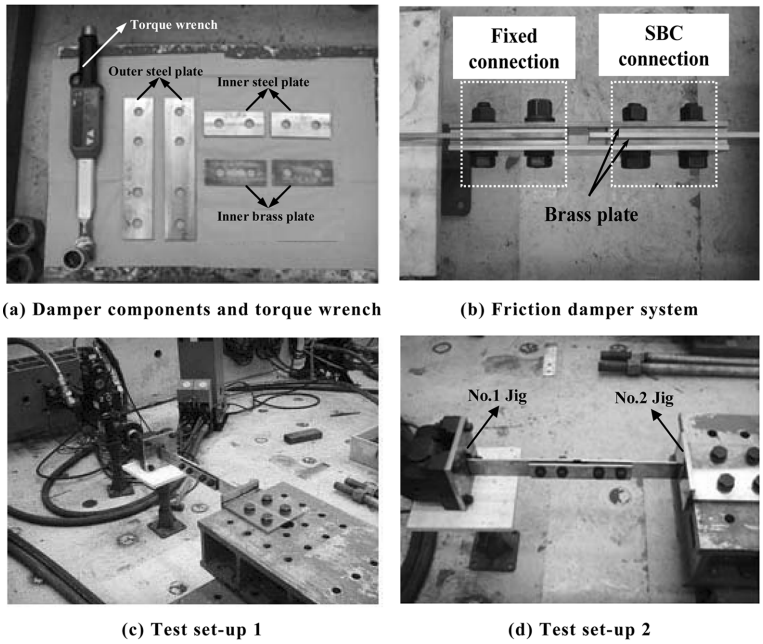

Fig. 1 SBC type friction damper system and test set-up

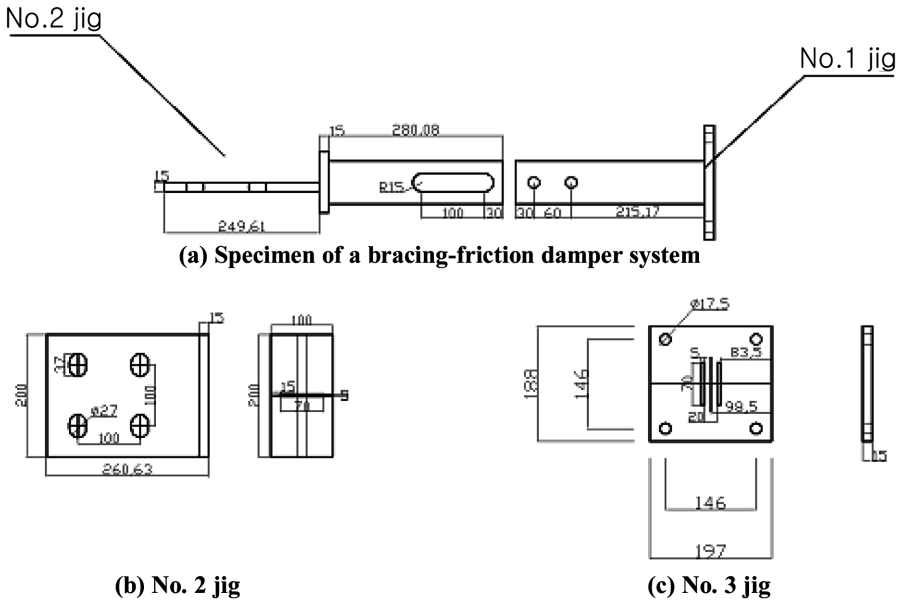

Fig. 2 Drawings of a test set-up

plates used as friction-inducing materials and a wrench that tightens the damper components by the specified value of a torque. The assembled damper system is shown in Fig. 1(b). The damper system was comprised of one inner steel plate and two outer brass and steel plates, as shown in the dotted circle part. Friction forces of the damper are produced in faying surfaces between brass and steel plates. Also,

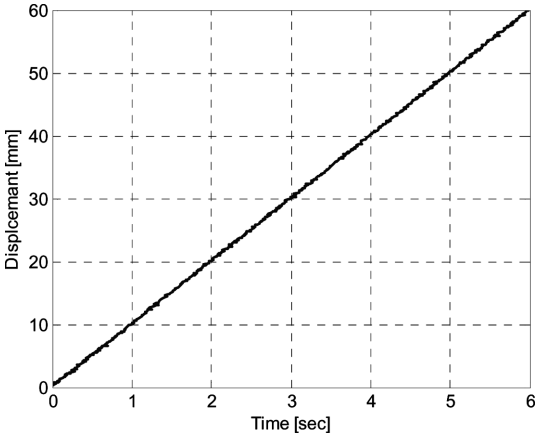

Fig. 3 Time history of monotonic load

contacting surfaces of these all plates that comprises the damper system were well grinded to keep constant slip loads after yielding.

Figs. 1(c) and (d) and Fig. 2 express a test set-up of the damper system and its drawings. Two jigs were welded at both sides of inner steel plates that would behave as a brace in a brace-friction damper system. The jig of No. 1 was connected to an actuator and the jig of No. 2 was fixed at the other end of the damper system to perform its uniaxial tests. Also, a teflon plate was inserted between an actuator and a supporting steel member to minimize a friction that might occurs during the tests, as shown in Figs. 1(c) and (d). Uniaxial loads generated by an actuator are transferred to the damper system through the inner plates, and then friction forces exerted by the damper system resist the external loads to statically equilibrate between them.

2.2. Monotonic loading test

For the test set-up and damper system addressed in the above explanation, monotonically increasing load tests were carried out for relating the torques applied to the damper system to its slip loads. Fig. 4

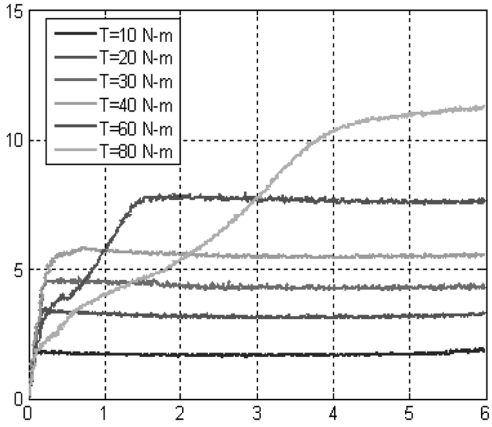

Fig. 4 Monotonic loads-displacements curves

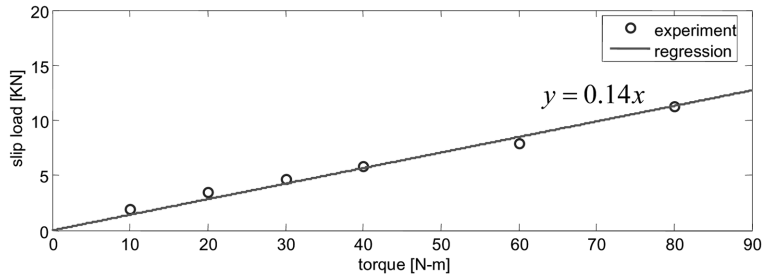

Fig. 5 Relation between torques and slip loads

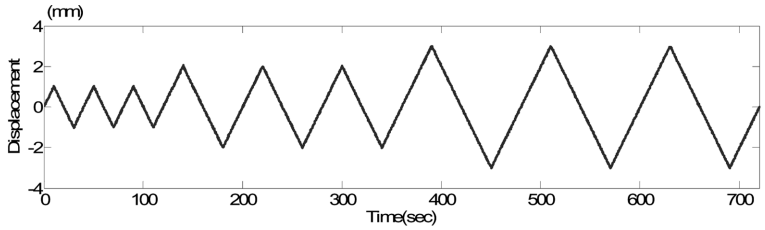

Fig. 6 Time history of cyclic load

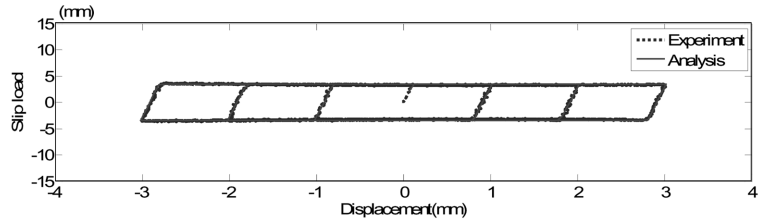

(a) T = 20 $N \cdot m$

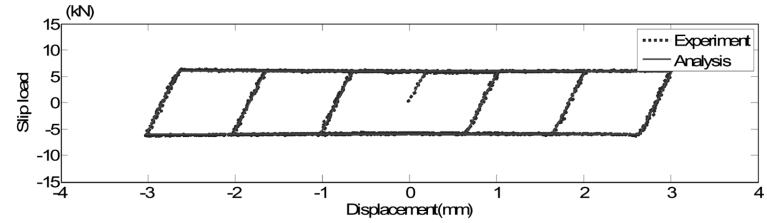

(b) T = 40 $N \cdot m$

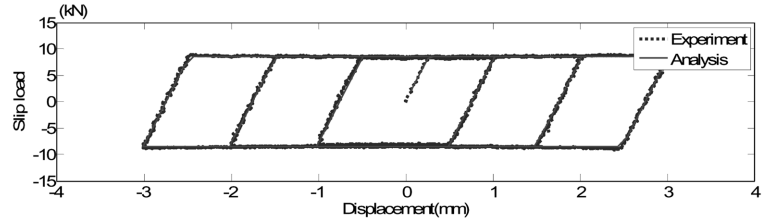

(a) T = 60 $N \cdot m$

Fig. 7 Cyclic loads-displacements curves

shows the corresponding loads – displacements curves along the applied torques for the slip loads, as the monotonic load such as Fig. 3 was applied to the damper system by an actuator that is driven by the displacement control with a loading rate of the 0.1 mm per second. It is observed from Fig. 4 that slip loads increase proportionally to the applied torques of the damper system while the slip load happens twice in the case of the torque of 60 N m and is obscure for the torque of 80 Nm. This is due to the buckling of a bracing member in the damper system subjected to a compressive loading during the test. Accordingly, in the followed cyclic loading tests of a damper system the buckling of a bracing member was suppressed by shortening the length of the inner steel plates, by which the SBC part is connected to jigs.

Based on the monotonic loading test results, we related the torques applied to the SBC part by a wrench to the slip loads of the friction damper system, as shown in Fig. 5. Using this linear relation between the torque and slip load, the prediction of slip loads could be practicable for the considering SBC type friction damper system.

2.3. Cyclic loading test

Slotted bolted connection type friction damper system was tested to investigate its energy dissipation characteristic for cyclic loads and to establish the numerical model for its hysteresis that will be discussed in the followed chapter. As shown in Fig. 6, a cyclic load that have the maximum amplitudes of 1, 2 and 3 mm and 3-repeated cycles over each sector was applied to the specimen by an actuator with the same loading rate as the previous monotonic loading test for various applied torques.

Fig. 7 shows the variation of the energy dissipation hysteresis of the damper system under consideration in this paper along for the alteration of experimentally applied torques (dotted line). The same tendency as the monotonic load testing results is observed from the figure; the growth of a slip load and thus the amount of a dissipation energy in the damper system according to the increase in a torque. It is also observed that a constant slip load was maintained over the repeated loading cycles, and the stable hysteretic behavior was obtained with the result that the contacting surfaces between the bracing and the brass plates were well treated by grinding them.

3. Numerical model of a friction damper system

A large percentage of energy dissipation devices is installed at inter-stories of building structures not by themselves but generally by using the additional supporting system that connects them to main structural members. Braces are most commonly used as supporting members of a SBC type friction damper system. Generally, one end of braces is fixed to a lower bare frame and the other end is connected to one end of a friction damper, and then the other end of a friction damper is fixed to an upper bare frame. Therefore, the brace and friction parts of a bracing-friction damper system under consideration herein are connected in series with each other, as shown in Fig. 8. k_b, δ, f_d and f_s are the

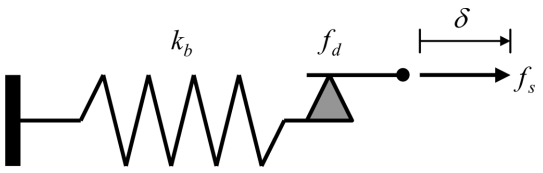

Fig. 8 Bracing-friction damper system

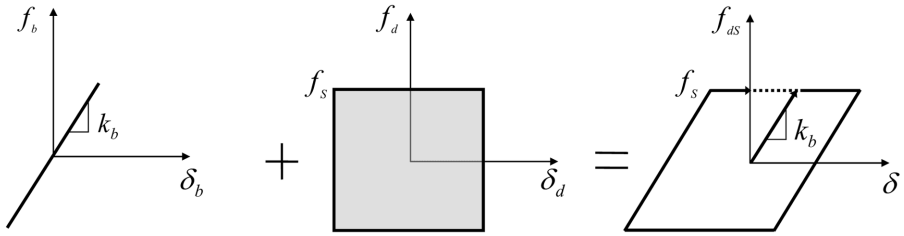

Fig. 9 Hysteretic loop of a braced damper system with a Coulomb friction element

stiffness of brace, inter story drift, frictional force exerted by the damper itself and the force applied to the entire bracing-friction damper system, respectively.

From the inspection of a numerical model such as Fig. 8, the force applied to a bracing-friction damper system, the frictional force in damper and the shear force in brace are mathematically equal with each other as follows:

$$f_s = f_d = k_b \delta_b \tag{1}$$

with the displacement constraint of the system that is represented by

$$\delta = \delta_b + \delta_d \tag{2}$$

where, δ_b and δ_d denote the displacements occurred in a brace and a damper, respectively.

The hysteretic loop of a bracing-friction damper system including a Coulomb friction element is expressed in Fig. 9 (Garcia and Soong 2002, Chopra 1995). In this loop, an arbitrary point over the hysteresis of a bracing-friction damper system satisfies the equilibrium of forces and boundary condition such as Eq. (1) and (2). Using this numerical model, the hysteresis loops of a bracing-friction damper system including the Coulomb friction element were numerically calculated for various slip loads, as denoted in Fig. 7 with straight lines. It is observed from Fig. 7 that the experimental and analytical hysteresis loops of the bracing-friction damper system under consideration are a good agreement with each other.

4. Numerical example

4.1. Building description

To compare the seismic performance of a damaged building structure with and without a bracing-friction damper system numerically modeled in the previous chapter, first a 10-story shear building was calculated herein.

Bi-linear model with 5% reduction in the secondary stiffness were assumed for the inter-story shear force and drift relation to represent the damaged building. The structural mass of 5×10^5 kg was equally distributed over all floors. The damping ratio of 5% in each mode was assumed to characterize the inherent damping of the building. The initial story stiffness varies from bottom to top with values, in the

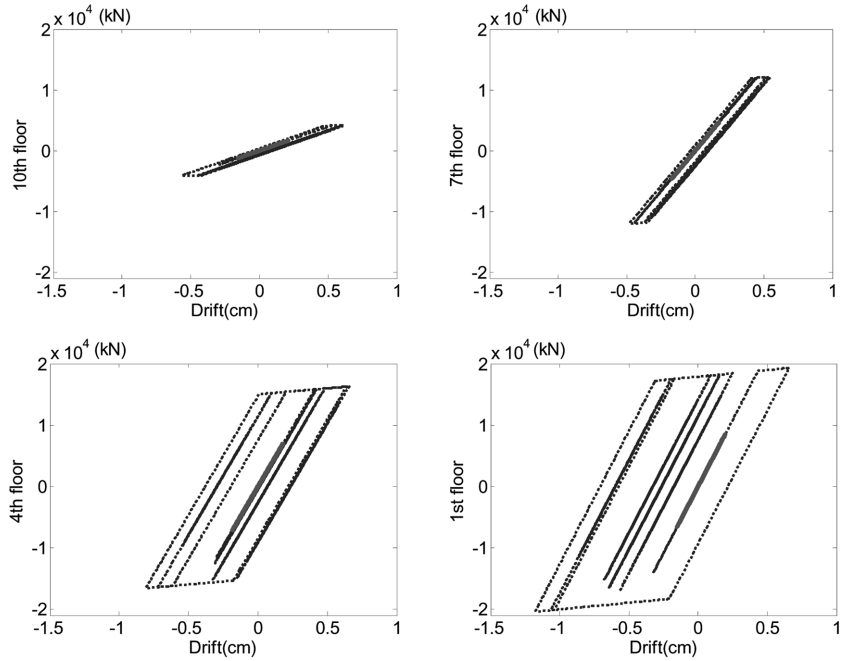

Fig. 10 Shear force-displacement characteristic

kN / m $\times 10^4$ units, as: 9.0, 8.9, 8.6, 8.1, 7.4, 6.6, 5.6, 4.4, 3.1 and 1.6. Also, the yielding load of a bare frame was set to vary from bottom to top with values, in the kN $\times 10^2$ units, as: 1.96, 1.86, 1.73, 1.65, 1.55, 1.42, 1.25, 1.03, 0.76 and 0.43. The equation of motion with these values for the structural properties is expressed by

$$\mathbf{M}\ddot{\mathbf{y}}(t) = \mathbf{C}\dot{\mathbf{y}}(t) + \mathbf{K_f}(t)\mathbf{y}(t) = -\mathbf{M1}\ddot{Y}_g(t) \tag{3}$$

where, $\mathbf{y}(t)$ and $\ddot{Y}_g(t)$ are the displacement vector relative to the ground and the ground acceleration, respectively. **M** and **C** are the structural mass and damping matrices, respectively. $\mathbf{K_f}(t)$ is the structural stiffness matrix that represents the non-linearity of bi-linear model. **1** is the unit column vector.

Eq. (3) was numerically calculated using Newmark method with the time interval of 0.001 sec and El Centro earthquake with the maximum amplitude of 340 gal as a ground acceleration. Fig. 10 shows the calculated inter-story shear force-drift characteristics of a bare frame under consideration in this study (dotted lines).

4.2. Bare frame retrofitted with bracing-friction damper system

The deployment of bracing-friction damper system numerically modeled early is discussed herein. The differential equation of the damaged building retrofitted with bracing-friction damper systems could be expressed by

$$\mathbf{M}\ddot{\mathbf{y}}(t) = \mathbf{C}\dot{\mathbf{y}}_s(t) + \mathbf{K_f}(t)\mathbf{y}_s(t) + \mathbf{F}_s(t) = -\mathbf{M1}\ddot{Y}_g(t) \tag{4}$$

where, $\mathbf{y}_s(t)$ is the displacement vector relative to the ground of a friction-damped building. $\mathbf{F}_s(t)$ is the restoring force vector exerted by the bracing-friction damper system such as Fig. 9, and thus could contain zero in the story where a bracing-friction damper system under consideration is not installed.

In this study, the ratio of the supporting bracing stiffness to story stiffness was fixed 2 for all stories. Also, the slip load normalized to maximum shear force was adopted to distribute it to each story. That is, two cases of distributions of a slip load according to stories were considered as follows:

Case 1: ρ_1 = slip load / maximum shear force of the undamped building.

Case 2: ρ_2 = slip load / maximum inter-story shear force of the undamped building.

Therefore, In Case 1 the same value of a slip load would be distributed over all stories for various ρ_1 value, while in Case 2 the different value of a slip load proportional of inter-story shear force would be imparted to each story for various ρ_2 value.

Also, the seismic performance of a damped building was evaluated using two kinds of indicies, as follows

$$R_d = \frac{\max\limits_{i=1,\ldots,n}\{|\delta_s(t)|_{\max}\}}{\max\limits_{i=1,\ldots,n}\{|\delta(t)|_{\max}\}} \qquad R_a = \frac{\max\limits_{i=1,\ldots,n}\{|\ddot{\mathbf{Y}}_s(t)|_{\max}\}}{\max\limits_{i=1,\ldots,n}\{|\ddot{\mathbf{Y}}(t)|_{\max}\}} \tag{5}$$

where, both R_δ and R_a denote the ratio of the damped response to undamped response. $\delta_s(t)$ and $\delta(t)$ represent the damped and undamped inter-story drifts, respectively. $\ddot{\mathbf{Y}}_s(t)$ and $\mathbf{Y}(t)$ are the damped and undamped absolute accelerations, respectively.

For these variables, Eq. (4) was repeatedly calculated using the same time interval and earthquake input motion applied for the undamped building. Fig. 11 shows the variation of the performance indicies defines as Eq. (5) according to the normalized slip load and slip load distributing method. It is observed that the slip load distribution of Case 2 is superior to Case 1 in reducing both the acceleration and drift response. The optimal normalized slip loads are found in $\rho_2 = 0.35$ for reducing the acceleration response and in $\rho_2 = 0.55$ for diminishing the inter-story drift response, respectively. Also, it is noted that an increasing the slip load beyond the optimal value could deteriorate the seismic performance for the damped acceleration response, and this trend is remarkable in the distribution method of slip load for Case 1.

Fig. 12 compares both the maximum acceleration and inter-story drift response reduction attained by the seismic designs with the value of $\rho_2 = 0.35$ and $\rho_2 = 0.55$ for Case 2 slip load distribution. It is

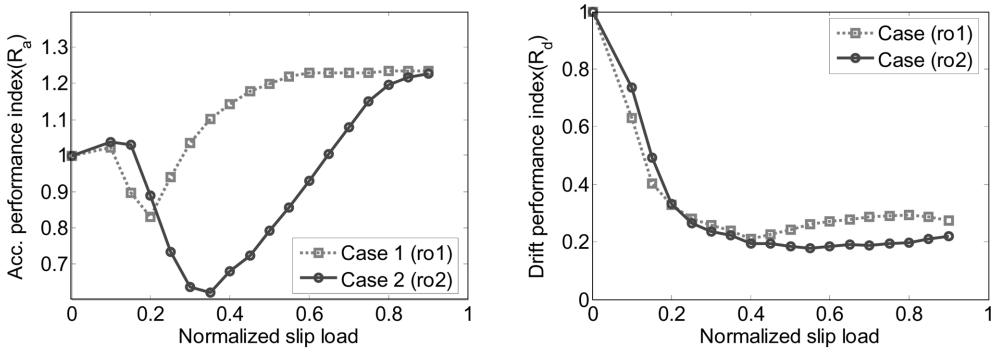

(a) Acceleration performance index (R_a) **(b) Drift performance index (R_d)**

Fig. 11 Variation of performance index according to the normalized slip load and slip load distribution

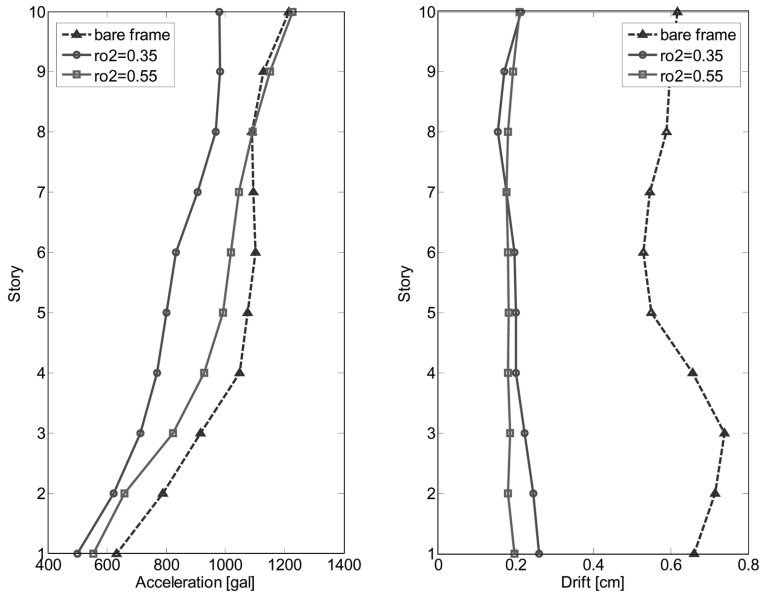

Fig. 12 Comparison of maximum response along the story for the Case 2 slip load distribution

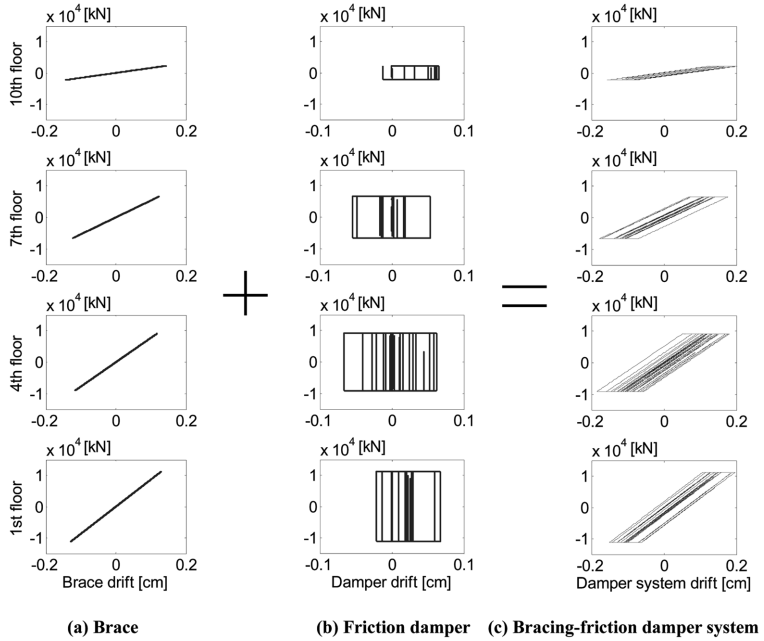

Fig. 13 Hyteretic behavior for the slip load of $\rho_2 = 0.55$

known that the friction damper system under consideration is more favorable in decreasing the drift response than the acceleration response reduction, since it is fundamentally installed at interstory of a building and directly controls the inter-story drift response. Also, it is observed that at the upper story of

damped building, the acceleration response by a seismic design for the value of $\rho_2 = 0.55$ that is not optimal value in reducing the acceleration response rather surpass that of undamped building.

Fig. 13 shows the hysteresis behavior of the brace, Coulomb friction damper and bracing-friction damper system designed for the slip load of $\rho_2 = 0.55$, respectively, at the different stories. It is known that the bracing-friction damper system under consideration exerted its energy dissipation efficiency at all stories of the damaged building, and as a result the damaged building was recovered to its linear state, as denoted in Fig. 10 with solid lines.

5. Conclusions

In this paper, the seismic design of the friction damper using performance indicies based on structural response was discussed in aspect of seismic retrofit of aged or damaged building structures. First, the Slotted Bolted Connection (SBC) type friction damper system that comprises steel braces and brass plates was manufactured and tested for monotonic and cyclic loads to investigate its energy dissipation characteristic. Test results were compared with numerical results based on the conventional bracing-friction damper model containing Coulomb friction element to evaluate its applicability to seismic retrofit of a damaged building. Then, the damper placement using this device was numerically investigated for applying it to the damaged-building assumed as a bi-linear model for its non-linearity of restoring force. Finally, the optimal slip load, which minimizes the given performance indicies based on structural response such as an acceleration and inter-story drift, was found and the efficacy of SBC type friction damper system under consideration was evaluated. Numerical results for the damaged building retrofitted with this slip load distribution showed that the seismic design of the bracing-friction damper system under consideration is effective for the structural response reduction especially such as the inter-story drift.

Acknowledgement

The authors would like to thank the Korea Science and Engineering Foundation(KOSEF) for their partial support of this work through Smart Infra-Structure Technology Center(SISTeC) at Korea Advanced Institute of Science and Technology(KAIST). Also, the work presented in this paper was supported by the Ministry of Construction & Transportation in Korea through the Industry and University Cooperative Research Program (Project No. C105A1050001-05A0505-00210) committed by the Korea Institute of Construction & Transportation Technology Evaluation and Plan (KICTTEP).

References

Chopra, A. K. (1995), *Dynamics of Structures; Theory and Applications to Earthquake Engineering*, Prentice Hall.

Consstantinou, M. C., Mokha, A. and Reinhorn, A. M. (1990), "Teflon bearings in base isolation. II: Modeling", *J. Struct. Eng.*, **116**(2), 455-474.

Filiatrault, A. and Cherry, S. (1990), "Seismic design spectra for friction-damped structures", *J. Struct. Eng.*, **116**, 1334-1355.

Fu, Y. and Cherry, S. (2000), "Design of friction damped structures using lateral force procedure", *Earthq. Eng.*

Struct. Dyn., **29**, 989-1010.
Garcia, D. L. and Soong, T. T. (2002), "Efficiency of a simple approach to damper allocation in MDOF structures", *J. Struct. Cont.*, **9**(1), 19-30.
Grigorian, C. E., Yang, T. and Popov, E. P. (1993), "Slotted bolted connection energy dissipators", *Earthq. Spectra*, **9**(3), 491-504.
Grigorian, C. E., Yang, T. S. and Popov, E. P. (1992), "Slotted bolted connection energy dissipators", Report of National Science Foundation, University of California, Berkeley.
Li, C. and Reinhorn, A. M. (1995), "Experimental and analytical investigation of seismic retrofit of structures with supplemental damping: Part II-friction devices", Technical Report NCEER-95-0009, State University of New York at Buffalo, Buffalo, NY.
Moreschi, L. M. and Singh, M. P. (2003), "Design of yielding metallic and friction dampers for optimal seismic performance", *Earthq. Eng. Struct. Dyn.*, **32**, 1291-1311.
Mualla, I. H. and Belev, B. (2002), "Performance of steel frames with a new friction damper device under earthquake excitation", *Eng. Struct.*, **24**, 365-371.
Pall, A. S. and Marsh, C. (1982), "Response of friction damped braced frames", *J. Struct. Eng.*, **108**(9), 1313-1323.
Soong, T. T. and Dargush, G. F. (1997), *Passive energy dissipation systems in structural engineering*, John Wiley & Sons.
Syrmakezis, C. A., Mavrouli, O. A. and Antonopoulos, A. K. (2006), "Rehabilitation of hospital buildings using passive control systems", *Smart Struct. Sys.*, **2**(4).
Viti, S., Cimellaro, G. P. and Reinhorn, A. M. (2006), "Retrofit of a hospital through strength reduction and enhanced damping", *Smart Struct. Sys.*, **2**(4).